Discreteness and resolution effects in rapidly rotating turbulence

Lydia Bourouiba[*]

McGill University, Montréal, Québec H3A 2K6, Canada

(Received 2 June 2008; published 25 November 2008)

Rotating turbulence is characterized by the nondimensional Rossby number Ro, which is a measure of the strength of the Coriolis term relative to that of the nonlinear term. For rapid rotation (Ro→0), nonlinear interactions between inertial waves are weak, and the theoretical approaches used for other weak (wave) turbulence problems can be applied. The important interactions in rotating turbulence at small Ro become those between modes satisfying the resonant and near-resonant conditions. Often, discussions comparing theoretical results and numerical simulations are questioned because of a speculated problem regarding the discreteness of the modes in finite numerical domains versus continuous modes in unbounded continuous theoretical domains. This argument finds its origin in a previous study of capillary waves, for which resonant interactions have a very particular property that is not shared by inertial waves. This possible restriction on numerical simulations of rotating turbulence to moderate Ro has never been quantified. In this paper, we inquire whether the discreteness effects observed in capillary wave turbulence are also present in inertial wave turbulence at small Ro. We investigate how the discreteness effects can affect the setup and interpretation of studies of rapidly rotating turbulence in finite domains. In addition, we investigate how the resolution of finite numerical domains can affect the different types of nonlinear interactions relevant for rotating inertial wave turbulence theories. We focus on Rossby numbers ranging from 0 to 1 and on periodic domains due to their relevance to direct numerical simulations of turbulence. We find that discreteness effects are present for the system of inertial waves for Rossby numbers comfortably smaller than those used in the most recent numerical simulations of rotating turbulence. We use a kinematic model of the cascade of energy via selected types of resonant and near-resonant interactions to determine the threshold of Ro below which discreteness effects become important enough to render an energy cascade impossible.

I. INTRODUCTION

Rotation affects the nonlinear dynamics of turbulent flows. The Rossby number is Ro=$U/2\Omega L$, with U a typical flow velocity, Ω the rotation rate, and L the characteristic length scale of the flow. It is the dimensionless ratio of the magnitude of the nonlinear term in the Navier-Stokes equation [$(\mathbf{u}\cdot\mathbf{\nabla})\mathbf{u}$, where $\mathbf{u}$ is the velocity vector] to the Coriolis term ($2\mathbf{\Omega}\times\mathbf{u}$, where $\mathbf{\Omega}$ is the rotation vector). When Ro=0, the Navier-Stokes equations in a rotating frame are linear and admit inertial wave solutions with anisotropic dispersion relation $\omega_{s_{\mathbf{k}}}=s_{\mathbf{k}}2\mathbf{\Omega}\cdot\mathbf{k}/|\mathbf{k}|$, where $s_{\mathbf{k}}=\pm$, and $\mathbf{k}$ is the wave number [1]. The modes with zero frequency $\omega_{s_{\mathbf{k}}}$ are modes that correspond to vertically averaged real-space velocity fields (for example, columnar vertically averaged modes aligned with the rotation axis). When Ro→0 three-dimensional isotropic rapidly rotating turbulent flows have been observed to generate two-dimensional columnar structures experimentally [2–4], and numerically in decay turbulence [5–7] and in forced turbulence [8–11].

When Ro→0, matched asymptotic expansion methods can be used for this weakly nonlinear problem. At first order in the expansion, energy transfers are restricted to interactions between triads of inertial waves that satisfy a condition of resonance [12]. Similar to other three-wave resonance systems, rotating turbulence with inertial waves is a system in which near-resonant interactions play an important role.

They were found to be responsible for the generation of an anisotropy observed [13].

When comparing simulations and experiments to theory, one should keep in mind that simulations and experiments are necessarily carried out in finite domains, whereas wave turbulence theories often assume an infinite domain. More specifically, numerical simulations usually assume periodic boundaries, and experiments are obviously carried out in bounded domains. In unbounded domains, the components of the wave vectors satisfying resonant and near-resonant conditions are real numbers, whereas they are restricted to the set of integers in bounded and periodic domains. This seemingly benign difference turns out to have major implications. In fact, Ref. [14] investigated the peculiar characteristics of several resonances (planetary waves, gravity waves, capillary waves, and drift waves in plasmas) satisfied only by integer wave number solutions in periodic domains. Reference [15] considered the existence of solutions for various wave systems including gravity, Rossby, and capillary waves and showed that capillary waves in a finite domain (integer-valued wave vector) cannot be resonant. Their resonance condition only has real-valued wave vector solutions. This kinematic result turns out to have major implications on the applicability of wave-turbulence results which are derived in infinite domains. In fact, several numerical studies showed that a sufficient level of nonlinearity is needed for the amplitudes of the capillary waves described by integer-valued wave vectors to overcome the discreteness and satisfy an approximate resonance, i.e., a near-resonance [16,17]. In other words, in a discrete domain, a sufficient threshold nonlinear broadening of the capillary wave resonance condition

*lydia.bourouiba@mail.mcgill.ca

is needed for the near-resonant conditions to generate nonlinear energy transfers. Below this threshold, the near-resonant interactions are not easily formed. Thus, given that no resonant interactions are possible, the energy cascade is stopped altogether. This regime is referred to as "frozen turbulence" [16]. Similar discreteness effects were also investigated for water waves [18–20]. Nazarenko [21,22] explicitly addressed the issue of applicability of wave turbulence (corresponding to the continuous wave number limit) to discrete wave number domains for the cases of water-wave and MHD turbulence, respectively.

The main distinction between inertial waves and capillary waves is that for the former, integer-valued wave number resonance solutions do exist. The resonant inertial wave interactions are thus always present in bounded and periodic domains. In contrast to capillary waves, there is no *a priori* need for a sufficient level of nonlinearity in order to trigger nonlinear energy transfers.

However, the dispersion relation of inertial waves can lead to complicated resonant surfaces. Therefore, a similar effect to that of frozen capillary wave turbulence effect could exist for inertial waves. If that was the case, the discreteness effect would be expected to reduce the possibility of energy transfers both via the resonant interactions alone or combined with near-resonant interactions. In fact, an effect of this nature has been speculated (although not verified). For example, Ref. [24] speculated that the use of numerical simulations for the study of small Ro flow could miss the slow mode dynamics.

Using decaying turbulence simulations, Bourouiba and Bartello [7] showed the existence of three rotating turbulent regimes. (1) A weakly rotating Rossby regime, for which the turbulent flow is not affected by rotation. (2) An intermediate Rossby regime characterized by a strong transfer of energy from the wave to the zero-frequency modes, with a peak at Ro ~ 0.2 [39]. (3) A small, or asymptotic Rossby regime, for which the zero-frequency modes receive less and less energy from the wave modes—tending to confirm decoupling theories. When forcing their simulations at intermediate scales, Ref. [13] speculated that their own simulations using Ro $=0.1$ guaranteed a sufficient nonlinear amplitude to allow for the capture of the near-resonant interactions while other simulations of Ref. [11] investigating a lower Ro, were not able to accurately capture the necessary near-resonant interactions. Thus, it was implied that the dynamics observed by Ref. [11] for their smaller Ro was a numerical artifact. Although Ref. [13] studied the effect of near-resonant interactions for Ro $\sim O(0.1)$, they did not quantify the effect of discreteness. Nevertheless, they did call for the need of doing this work: "although the latter statement [capturing the near-resonances in finite domains] begs to be quantified, such a study is beyond the scope of the present paper."

The finite domain effect on rapidly rotating flows is inherent to both numerical and experimental studies, yet studying such an effect using experiments is delicate. One could envision comparing statistics obtained in a series of different sized rotating tanks. However, Ro at which the asymptotic theories apply (found to be, for example, Ro $=0.01$ in Ref. [25]) are considerably smaller than those typical of rotating tank experiments (for example, Ro $=2$ was the lowest Rossby

TABLE I. Properties of the interactions of interest contributing to the energy transfers.

Type of triad	Resonant (R) and/or Near-resonant (N):	
	$0 < \text{Ro} \ll 1$	Ro $=0$
$22 \rightarrow 2$	R	R
$33 \rightarrow 2$	N with $C_{33 \rightarrow 2} \neq 0$	vanishes with $C_{33 \rightarrow 2} = 0$
$23 \rightarrow 3$	R and N	R catalytic: no energy transfer to the 2D mode
$33 \rightarrow 3$	R and N	R: energy transfer to the 3D mode with smallest $\omega_{s_\mathbf{k}}$

number obtained in experiment of Ref. [26]). The difficulty is that boundary layer effects quickly become important when rotation rates are high (Ref. [27], for example). Moreover, in a more recent study, the confinement effect was argued to inevitably generate inhomogeneous turbulence (see Ref. [28]). A possible alternative to rotating tanks is the setup used by Ref. [29], in which a flow of air was passing through a large rotating cylinder and a dense honeycomb. This produces elongated structures which could be less affected by boundary layers and inhomogeneity effects. Isolating the discreteness effects could be possible in such a setting in which dominant boundary layer effects could be reduced.

We now focus on the discreteness effects in numerical domains. In particular, our goal is to clarify this issue and to investigate how the reduction of Ro affects the distribution and number of resonant and near-resonant interactions as Ro$\rightarrow 0$ in periodic domains. When carrying out and interpreting the results of simulations of rotating turbulence, there are two aspects to the discreteness effect. The first is the difference between bounded and unbounded domains in general. Unbounded domains lead to real-valued wave numbers in spectral space. Bounded and periodic domains lead to integer-valued wave numbers. The second is related to the spatial resolution of a given bounded domain of interest. When a bounded domain of interest is selected, the spatial resolution determines the truncation wave number. We inquire whether a discreteness effect leading to a phenomenon similar to the "frozen turbulence" observed with capillary waves is also present here with inertial waves. In addition, we investigate how the resolution affects the different types of interactions relevant for rotating inertial wave turbulence theories (see Table I).

We find that discreteness effects are present for the system of inertial waves. We quantify the minimum nonlinear broadening Rossby number Ro$_{min}$ below which the domain does not contain interactions coupling the zero-frequency two-dimensional (2D) modes to the 3D inertial wave modes. Thus, a regime of decoupling would be observed for simulations with Ro $<$ Ro$_{min}$. We also find the critical nonlinear broadening Ro$_c$ below which the theories predicting the freezing of vertical transfers in inertial wave turbulence would be observed in bounded domains. Finally, given a domain of interest for numerical simulations, we investigate whether a freezing of the energy cascade is present for iner-

tial waves and find this to be the case. We quantify the threshold nonlinear broadening Ro_f below which such a freezing occurs. This is done for various resolutions. This freezing of the energy cascade is found to be an inherent property of bounded systems. Our results can allow a more accurate interpretation and comparison of the results obtained in bounded domains with the results derived in unbounded domains. In particular, our results also aim at improving the setup of future numerical simulations of rapidly rotating turbulence.

First, the notation used to classify the various types of interactions are presented in Sec. II. The properties of the interactions and their interaction coefficients are recalled. In Sec. III, the number of near-resonant interactions and resonant interactions are quantified as a function of the nonlinear broadening and the truncation wave numbers. In Sec. IV, we investigate the effect of the nonlinear broadening on the capacity of the resonant and near-resonant interactions to generate a propagation of energy transfers to all the modes of the model. Threshold values of nonlinear broadening are obtained for various resolutions. In Sec. V we discuss the results obtained in the light of recent dynamical numerical simulations of rotating turbulent flows.

II. MODAL DECOMPOSITION AND TYPES OF INTERACTIONS

We focus on a triply periodic domain as it is the domain most relevant for direct numerical simulations of homogeneous turbulence. In a triply periodic domain of size $L \times L \times L$ the velocity field of an incompressible fluid can be represented by a Fourier series

$$\mathbf{u}(\mathbf{r},t) = \sum_{\mathbf{k}} \mathbf{u}(\mathbf{k},t)e^{i\mathbf{k}\cdot\mathbf{r}}, \tag{1}$$

where $\mathbf{r} = (x,y,z)$ is the position vector in real-space with three components $i = \sqrt{-1}$, $\mathbf{k} = \Delta_k(k_x, k_y, k_z)$, with $\Delta_k = 2\pi/L$, and with $k_{x,y,z}$ integer wave numbers taking the values $0, \pm 1, \pm 2, \ldots$. The continuity equation in Fourier space is $\mathbf{u}(\mathbf{k}) \cdot \mathbf{k} = 0$.

Solutions of the linear rotating flow equations (with Ro $= 0$) can be expressed as a superposition of inertial waves with nondimensional inertial frequencies

$$\omega_{s_{\mathbf{k}}} = s_{\mathbf{k}}\hat{\mathbf{z}} \cdot \mathbf{k}/|\mathbf{k}|, \tag{2}$$

where $s_{\mathbf{k}} = \pm$, and $\hat{\mathbf{z}}$ is the unit vector for the direction corresponding to the rotation axis. (See Ref. [1] for details.) The inertial waves turn out to have the same structure as the helical modes (eigenmodes of the curl operator), which are defined as [1,30]

$$\mathbf{N}^{s_{\mathbf{k}}} = \left(\frac{\hat{\mathbf{z}} \times \mathbf{k}}{|\hat{\mathbf{z}} \times \mathbf{k}|} \times \frac{\mathbf{k}}{|\mathbf{k}|} + is_{\mathbf{k}}\frac{\hat{\mathbf{z}} \times \mathbf{k}}{|\hat{\mathbf{z}} \times \mathbf{k}|} \right). \tag{3}$$

When Ro is small but nonzero, a two-time-scale asymptotic expansion can be performed with a fast time scale $\tau_0 = t$ associated with the rotation time scale, and a slow time scale $\tau_1 = \text{Ro } t$ associated with the nonlinearity. The velocity field becomes

$$\mathbf{u}(\mathbf{k},\tau_0,\tau_1) = \sum_{s_{\mathbf{k}}=\pm} A_{s_{\mathbf{k}}}(\mathbf{k},\tau_1)\mathbf{N}^{s_{\mathbf{k}}}(\mathbf{k})e^{i\omega_{s_{\mathbf{k}}}\tau_0}. \tag{4}$$

When carrying the expansion to the second order [1,31] the equation governing the evolution of the amplitudes $A_{s_{\mathbf{k}_1}}$ is obtained. The nonlinear interactions are restricted to interactions between modes $(\mathbf{k}_1, \mathbf{k}_2, \mathbf{k}_3)$ satisfying the *resonant* condition

$$\omega_{s_{\mathbf{k}_1}} + \omega_{s_{\mathbf{k}_2}} + \omega_{s_{\mathbf{k}_3}} = 0, \quad \mathbf{k}_1 + \mathbf{k}_2 + \mathbf{k}_3 = 0. \tag{5}$$

The nonlinear interactions that are resonant are thus the interactions contributing on the long-time scale τ_1 to the long-term evolution of the wave amplitudes; omitting viscosity:

$$\partial_{\tau_1} A_{s_{\mathbf{k}_1}}(\mathbf{k}_1,\tau_1) = -\frac{1}{4}\text{Ro} \sum_{\substack{\mathbf{k}_1+\mathbf{k}_2+\mathbf{k}_3=0 \\ s_{\mathbf{k}_1},s_{\mathbf{k}_2}}}^{\omega_{s_{\mathbf{k}_1}}+\omega_{s_{\mathbf{k}_2}}+\omega_{s_{\mathbf{k}_3}}=0} C^{s_{\mathbf{k}_2}s_{\mathbf{k}_3}s_{\mathbf{k}_1}}_{\mathbf{k}_2\mathbf{k}_3\to\mathbf{k}_1}$$

$$\times A^*_{s_{\mathbf{k}_2}}(\mathbf{k}_2,\tau_1)A^*_{s_{\mathbf{k}_3}}(\mathbf{k}_3,\tau_1), \tag{6}$$

where $C^{s_{\mathbf{k}_2}s_{\mathbf{k}_3}s_{\mathbf{k}_1}}_{\mathbf{k}_2\mathbf{k}_3\to\mathbf{k}_1}$ is the interaction coefficient of the triad $(\mathbf{k}_1, \mathbf{k}_2, \mathbf{k}_3)$ that contributes to the equation governing the amplitude of the mode $\mathbf{k}_1$. Reference [30] showed that

$$C^{s_{\mathbf{k}_2}s_{\mathbf{k}_3}s_{\mathbf{k}_1}}_{\mathbf{k}_2\mathbf{k}_3\to\mathbf{k}_1} = (s_{\mathbf{k}_2}k_2 - s_{\mathbf{k}_3}k_3)(N^{*s_{\mathbf{k}_2}} \times N^{*s_{\mathbf{k}_3}}) \cdot N^{*s_{\mathbf{k}_1}}. \tag{7}$$

Each interacting triad satisfying $\mathbf{k}_1 + \mathbf{k}_2 + \mathbf{k}_3 = 0$ conserves energy and helicity implying that

$$C^{s_{\mathbf{k}_3}s_{\mathbf{k}_2}s_{\mathbf{k}_1}}_{\mathbf{k}_3\mathbf{k}_2\to\mathbf{k}_1} + C^{s_{\mathbf{k}_1}s_{\mathbf{k}_3}s_{\mathbf{k}_2}}_{\mathbf{k}_1\mathbf{k}_3\to\mathbf{k}_2} + C^{s_{\mathbf{k}_1}s_{\mathbf{k}_2}s_{\mathbf{k}_3}}_{\mathbf{k}_1\mathbf{k}_2\to\mathbf{k}_3} = 0 \tag{8a}$$

and

$$s_{\mathbf{k}_1}k_1 C^{s_{\mathbf{k}_3}s_{\mathbf{k}_2}s_{\mathbf{k}_1}}_{\mathbf{k}_3\mathbf{k}_2\to\mathbf{k}_1} + s_{\mathbf{k}_2}k_2 C^{s_{\mathbf{k}_1}s_{\mathbf{k}_3}s_{\mathbf{k}_2}}_{\mathbf{k}_1\mathbf{k}_3\to\mathbf{k}_2} + s_{\mathbf{k}_3}k_3 C^{s_{\mathbf{k}_1}s_{\mathbf{k}_2}s_{\mathbf{k}_3}}_{\mathbf{k}_1\mathbf{k}_2\to\mathbf{k}_3} = 0. \tag{8b}$$

We decomposed the modes into two categories: the modes corresponding to the nonzero inertial waves (with $k_z \neq 0$), denoted 3 or 3D,

If $\mathbf{k} \in W_{\mathbf{k}} = \{\mathbf{k} | k \neq 0 \text{ and } k_z \neq 0\}$ then $\mathbf{u}(\mathbf{k}) = \mathbf{u}_{3D}(\mathbf{k})$ $\tag{9}$

and the modes with a null inertial wave frequency (with $k_z = 0$), denoted 2 or 2D, which correspond to a real-space velocity field that is averaged vertically

If $\mathbf{k} \in V_{\mathbf{k}} = \{\mathbf{k} | k \neq 0 \text{ and } k_z = 0\}$ then $\mathbf{u}(\mathbf{k}) = \mathbf{u}_{2D}(\mathbf{k}_h)$, $\tag{10}$

where $k_h = \sqrt{k_x^2 + k_y^2}$ is the horizontal wave number. The total energy $E = \frac{1}{2}\Sigma_{\mathbf{k}}|\mathbf{u}(\mathbf{k})|^2$ becomes $E = E_{2D} + E_{3D}$, with

$$E_{2D} = \frac{1}{2}\sum_{\mathbf{k}\in V_{\mathbf{k}}} |\mathbf{u}_{2D}(\mathbf{k})|^2, \quad E_{3D} = \frac{1}{2}\sum_{\mathbf{k}\in W_{\mathbf{k}}} |\mathbf{u}_{3D}(\mathbf{k})|^2. \tag{11}$$

Using Eqs. (9) and (10), the nonlinear interactions between triads in Eq. (6) can be classified as $(33 \to 2)$, $(23 \to 3)$, $(33 \to 3)$, and $(22 \to 2)$, detailed in Table I. The notation $(jk \to i)$ stands for interaction between modes j, k, and i contrib-

uting to the equation of evolution for the mode i, with an interaction coefficient $C_{jk \to i}^{s_j, s_k, s_i} \neq 0$. It is symmetric in j and k.

In the Ro$\to 0$ limit, where the two-timescale expansion is valid, only the resonant interactions satisfying Eq. (5) make a significant contribution to the nonlinear energy transfers. The interactions $22 \to 2$ are all trivially resonant. The resonant interactions $33 \to 2$ were shown by Waleffe [31] to have no contribution to the energetic of the 2D modes. That is, if $(\mathbf{k}_1, \mathbf{k}_2, \mathbf{k}_3)$ is a resonant triad, with $(\mathbf{k}_2, \mathbf{k}_3) \in W_{\mathbf{k}}$ and $\mathbf{k}_1 \in V_{\mathbf{k}}$, then the interaction coefficient $C_{\mathbf{k}_3 \mathbf{k}_2 \to \mathbf{k}_1}^{s_{\mathbf{k}_3}, s_{\mathbf{k}_2}, s_{\mathbf{k}_1}} = 0$, and the two other interacting coefficients satisfy $C_{\mathbf{k}_1 \mathbf{k}_2 \to \mathbf{k}_3}^{s_{\mathbf{k}_1}, s_{\mathbf{k}_2}, s_{\mathbf{k}_3}} = -C_{\mathbf{k}_3 \mathbf{k}_1 \to \mathbf{k}_2}^{s_{\mathbf{k}_3}, s_{\mathbf{k}_1}, s_{\mathbf{k}_2}}$ [from Eq. (8a)]. The resonant interactions $32 \to 3$ are referred to as catalytic. If this property is combined with our definition of interaction $ij \to k$ as an interaction with $C_{ij \to k}^{ijk} \neq 0$, then the resonant interactions $33 \to 2$ do not exist (are inactive). The energy spectra equations accounting only for resonant interactions can then be written as

$$\frac{\partial E_{3D}}{\partial t}(\mathbf{k} \in W_{\mathbf{k}}, t) = (T_{33 \to 3\text{res}} + T_{32 \to 3\text{res}})(\mathbf{k} \in W_{\mathbf{k}}, t),$$

(12)

$$\frac{\partial E_{2D}}{\partial t}(\mathbf{k} \in V_{\mathbf{k}}, t) = T_{22 \to 2\text{res}}(\mathbf{k} \in V_{\mathbf{k}}, t),$$

(13)

where T represents the Fourier-space energy transfer terms and the term $T_{33 \to 2\text{res}} = 0$ does not appear. Note that in contrast to the resonant $33 \to 2$, the near-resonant interactions $33 \to 2$ are active. They exchange energy with the 2D modes, i.e., $C_{33 \to 2}^{s_3 s_3 s_2} \neq 0$. The near-resonant interactions denoted $33 \to 2$ and $32 \to 3$ are essentially denoting the same active triads.

The resonant $33 \to 2$ property is at the origin of the decoupling theories, which predict a decoupling between the inertial waves and the two-dimensional coherent structures in a rapidly rotating flow. This is coherent with the work of Ref. [32,33], who averaged the equations and separated the fast waves and the slow modes. They obtained an equation governing the vertically averaged 2D structures of the flow decoupled from the wave dynamics in the limit of small Ro. However, Ref. [34] later argued that for an unbounded domain, coupling terms between the 2D and the wave modes remain active even at Ro=0. That is, no decoupling is achievable in unbounded domains.

Concerning the 3D dynamics governed by Eq. (12), the resonant $33 \to 3$ interactions transfer energy to the $W_{\mathbf{k}}$ mode of the triad with the lowest frequency $\omega_{s_{\mathbf{k}}}$ [31]. Cambon *et al.* [24] observed an inhibition of the overall energy transfers (including both 2D and 3D modes), but no inverse cascade. They argued that an inverse cascade could only be achieved by resonant interactions. Using a closure model, they later confirmed the tendency of the resonant interactions to transfer energy toward the slow frequency modes [23]. Another dynamics was proposed for the resonant 3D modes. Reference [33] suggested that more $32 \to 3$ resonant interactions are possible compared to the numbers of $33 \to 3$. As a result,

energy transfers in Eq. (12) would be dominated by $32 \to 3$ interactions and this would lead to a reduced vertical 3D energy transfers as Ro$\to 0$.

Using a kinematic approach, Ref. [35] showed that near-resonant interactions in discrete domains are much more numerous than exact resonances in three-wave interaction systems—inertial waves are an example of such a three-wave resonant interaction system. This is not necessarily the case for four- (and more)-wave interaction systems, where the number of exact-resonances in a discrete domain can be very large even in small spectral domains. The results of the forced numerical simulations of rotating turbulence in periodic domains by Ref. [13] showed that the near-resonant interactions satisfying an approximate resonance modeled by

$$|\omega_{s_{\mathbf{k}_1}} + \omega_{s_{\mathbf{k}_2}} + \omega_{s_{\mathbf{k}_3}}| \lesssim \text{Ro}, \quad \mathbf{k}_1 + \mathbf{k}_2 + \mathbf{k}_3 = \mathbf{0} \quad (14)$$

played an important role in the energy transfers at moderately small values of Ro. Note that here, the frequencies $\omega_{s_{\mathbf{k}}}$ are nondimensional as defined in Eq. (2). The small parameter Ro in Eq. (14) is the nonlinear broadening of the resonant interaction. It depends on the spectrum of the flow and the level of nonlinearity of the turbulence for the scales associated with the interacting triads. Recall that due to the dispersion relation of capillary waves, Ref. [15] showed that only near-resonant interactions are possible in a discrete domain. In an unbounded domain, both resonances and near-resonances would contribute to nonlinear transfers. In contrast to capillary waves, inertial wave modes can be both exact resonances (5) and near resonances (14) in both a discrete and continuous spectral domain.

III. NUMBER OF EXACT AND NEAR-RESONANCES

As a first step in evaluating the influence of the (1) discreteness and the (2) resolution effects, we consider a range of spectral domains corresponding to a fixed size $L \times L \times L$ but with various spatial resolutions $N^3 \approx 64^3, 100^3, 133^3, 150^3, 166^3$. These correspond to spectral truncation wave numbers of $k_t \approx 21, 33, 50, 55$ ($k_t \approx N/3$ for dealiasing [36]). Due to the anisotropy of the inertial dispersion relation (2), we consider a spectral domain with a cylindrical truncation such that $\max(|k_z|) = k_{\max}$, and $\max(k_h) = k_{\max}$. We ignore the range of modes corresponding to the dissipation range $k_d < k < k_t$. Assuming that $k_d \approx 0.9 k_t$, we only consider the modes of the spectral domain with $|k_z| \leq k_{\max}$ and $k_h \leq k_{\max}$, with $k_{\max} = 20, 30, 40, 45, 50$.

To give some perspective we recall that the numerical studies of rotating turbulence performed by Ref. [8] were obtained in a 32^3 numerical domain which would correspond to $k_t = 10$. Simulations of Ref. [13] used a resolution of 64^3, which correspond to $k_t = 21$. Simulations of Refs. [10,11] used resolutions of 128^3, which correspond to $k_t = 42$. Reference [7] used resolutions of 100^3 and 200^3, which correspond to $k_t = 33$ and 66. The recent large-scale forcing simulations of Ref. [37] used a resolution of 512^3, which correspond to $k_t = 170$.

We counted the number of interactions satisfying Eq. (14) for a fixed domain size with varying truncation numbers cor-

responding $k_{max}=20,30,40,45,50$. For each triad, we consider the eight possible types of interactions defined by $(s_{\mathbf{k}_1}, s_{\mathbf{k}_2}, s_{\mathbf{k}_3})$. We summarize in Table I the type of interactions on which we focus. When calculating the number of $(3_a 3_b \rightarrow 3_c)$ and $(2_a 2_b \rightarrow 2_c)$ interactions, we only consider the interactions with all three non-null interacting coefficients $(C_{3_a 3_b \rightarrow 3_c}^{s_3 s_3 s_3}, C_{3_b 3_c \rightarrow 3_a}^{s_3 s_3 s_3}, C_{3_a 3_c \rightarrow 3_b}^{s_3 s_3 s_3})$ and $(C_{2_a 2_b \rightarrow 2_c}^{s_2 s_2 s_2}, C_{2_b 2_c \rightarrow 2_a}^{s_2 s_2 s_2}, C_{2_a 2_c \rightarrow 2_b}^{s_2 s_2 s_2})$, respectively. The $32 \rightarrow 3$ interactions are those with at most one zero interaction coefficient. The $3_a 3_b \rightarrow 2$ are restricted to the interactions with $C_{3_a 3_b \rightarrow 2}^{s_3 s_3 s_2} \neq 0$. In other words, the number of $32 \rightarrow 3$ contains both resonances and near-resonances, whereas the $33 \rightarrow 2$ are only near-resonances.

Figure 1 shows the resulting numbers of $33 \rightarrow 3$, $33 \rightarrow 2$, and $32 \rightarrow 3$ satisfying Eq. (14) for a range of nonlinear broadening Ro between 0 and 1. The number of $33 \rightarrow 2$ and the $33 \rightarrow 3$ interactions (top and lower panels) both show a decrease with Ro until they reach a plateau for small Ro, whereas, $33 \rightarrow 2$ (middle panel) near-resonances decrease with Ro and vanish for sufficiently small Ro.

As the nonlinear broadening is decreased, the number of $33 \rightarrow 3$ interactions reaches a nonzero plateau that varies with the truncation wave number considered. This plateau corresponds to the number of exactly resonant interactions satisfying Eq. (5). The number of $33 \rightarrow 3$ resonances varies from $R_{33 \rightarrow 3}=232$ for $k_{max}=20$ to $R_{33 \rightarrow 3}=7408$ for $k_{max}=50$. This remains quite small compared to the number of near-resonances $N_{33 \rightarrow 3}$ obtained for higher values of nonlinear broadening. This latter increases rapidly with Ro and this is true for all truncations. For example, for a truncation of $k_{max}=20$, the number of near-resonances $N_{33 \rightarrow 3}$ increases dramatically from 704 (for Ro$=1 \times 10^{-7}$) to 7.43×10^8 (for Ro$=0.8$). The plateau corresponding to the number of exact-resonances followed by a rapid increase of the number of near-resonances as Ro increases is reminiscent of the results obtained for near-resonant surface gravity waves in Ref. [18]. They found that the number of near-resonances reaches a nonzero plateau as their nonlinear broadening decreased. However, the number of resonant interactions on the plateau was found to be sufficiently large to preclude a regime similar to capillary wave "frozen" turbulence.

The decoupling between the 3D and 2D modes was predicted by decoupling theories derived in continuous domains for Ro infinitesimally small. These theories rely on the vanishing coupling coefficient between the 2D and the 3D modes in the $33 \rightarrow 2$ interactions, leading to decoupled Eqs. (12) and (13). In other words, we know that in unbounded domains $C_{33 \rightarrow 2} \rightarrow 0$ as Ro$\rightarrow 0$ implies a decoupled dynamics. However, in bounded domains the Ro for which these theories would apply is finite and undetermined.

We counted the number of $33 \rightarrow 2$ near-resonances in a given bounded domain. Figure 1 shows clearly that there is a minimum finite nonlinear broadening, below which the $33 \rightarrow 2$ interactions vanish. We will refer to this minimum as Ro$_{min}$. It varies with the resolution used. Ro$_{min}$ changes from Ro$_{min}=6.6 \times 10^{-5}$ at spectral truncation $k_{max}=20$ to Ro$_{min}=3.3 \times 10^{-6}$ for a truncation of $k_{max}=50$. For Ro$<$Ro$_{min}$ the only interactions between the $V_{\mathbf{k}}$ and the $W_{\mathbf{k}}$ modes are those labeled $32 \rightarrow 3$, which become catalytic, resulting in a decou-
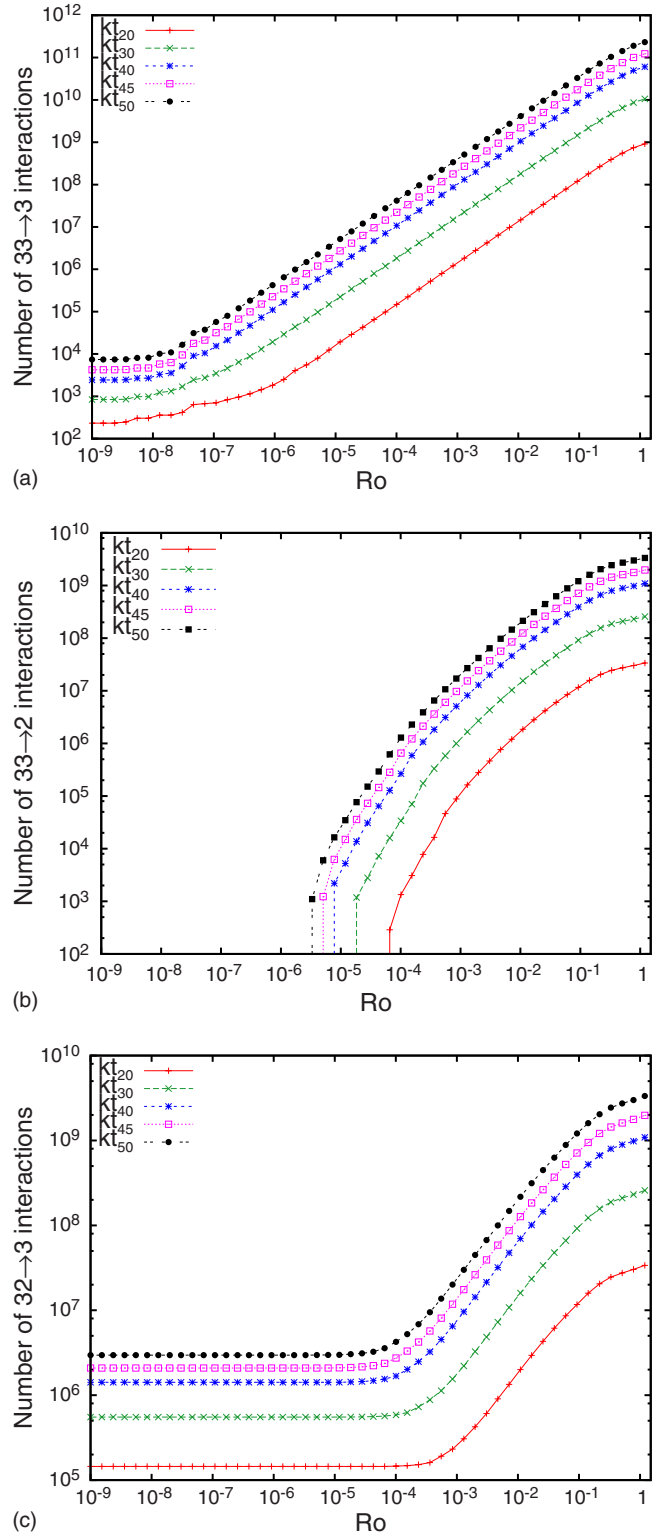

FIG. 1. (Color online) Total number of active resonant and near-resonant $33 \rightarrow 3$, $33 \rightarrow 2$ and $23 \rightarrow 3$ [see Table I and Eq. (14)] as a function of nonlinear broadening Ro and the spatial resolutions used.

pling between the 2D and the 3D dynamics. Recall that for Ro$<$Ro$_{min}$, the catalytic interactions do not exchange energy between scales. Although, they do redistribute the 3D energy horizontally [between various (k_x, k_y) modes of fixed k_h]. Fi-
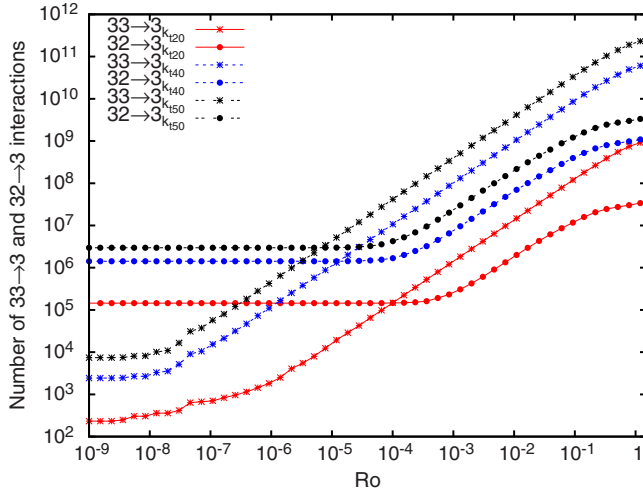
FIG. 2. (Color online) Comparison of the number of resonant and near-resonant interactions $33 \rightarrow 3$ and $32 \rightarrow 3$ as a function of the nonlinear broadening and the truncation of the spectral domain used.

nally, the values of Ro_{min} (from Fig. 1) are far lower than Rossby numbers found in the literature on numerical simulations of rotating turbulence. For example, with a resolution of 128^3—with a maximum wave number close to 40—numerical simulations performed with a nonlinear broadening of $Ro < Ro_{min} = 7.8 \times 10^{-6}$ would automatically produce a decoupling between 3D and 2D modes. For $Ro > Ro_{min}$, near-resonances transferring energy between 2D and 3D modes are still present, hence, if a decoupling is observed numerically at these Rossby numbers, it is an intrinsic dynamical property of the flow as opposed to being due to a lack of capture of key interactions by the numerical domain.

In the context of resonant interaction theories, Ref. [33] suggested that reduced vertical energy transfers would be observed. The reason for this lies with the assumption that the number of exact resonances $R_{32 \rightarrow 3}$ would be greater than $R_{33 \rightarrow 3}$. A similar stalling of vertical transfers was predicted and observed for weak Alfvén turbulence [38]. These predictions contrast with the results suggesting the creation of anisotropy by the predominant resonances $33 \rightarrow 3$ transferring energy toward modes with small frequencies $\omega_{s_\mathbf{k}}$.

Figure 2 shows that both dynamics exist. In one case, the $33 \rightarrow 3$ are dominant and in the other, the $32 \rightarrow 3$ are dominant. A critical nonlinear broadening, Ro_c, delimits the two cases. For $Ro < Ro_c$, the number of $33 \rightarrow 3$ near-resonances $N_{33 \rightarrow 3}$ is smaller than the number of $32 \rightarrow 3$ near-resonances $N_{32 \rightarrow 3}$. For $Ro > Ro_c$, $N_{33 \rightarrow 3} > N_{32 \rightarrow 3}$. Ro_c is a function of the truncation wave number. The higher the k_t, the smaller the Ro_c. For $Ro < Ro_c$, the reduction of vertical energy transfers discussed in Ref. [33] could be observable in bounded domains, whereas for $Ro > Ro_c$, the dominant number of $33 \rightarrow 3$ lead to energy transfers toward the modes with smaller frequencies $\omega_{s_\mathbf{k}}$.

We find that $Ro_c < Ro_{min}$ for all the k_{max} used here. This implies that for a nonlinear broadening of $Ro < Ro_c < Ro_{min}$, the interscale energy transfers in a given simulation would be due to the relatively small number of $33 \rightarrow 3$ interactions. For example, in the case of $k_t = 20$, for $Ro = 10^{-6} < Ro_c < Ro_{min}$,

we have $N_{33 \rightarrow 2} = O(10^3)$. As a result, if one is interested in the small Ro limit, the question becomes whether resonances, even in these small numbers, are sufficient to guarantee that energy transfers occur in such bounded domains.

In a continuous spectral space truncated at k_t, the number of $33 \rightarrow 3$ interactions are expected to increase with $\sim k_t^6$ with the truncation wave number. Similarly, the number of $32 \rightarrow 3$ and $33 \rightarrow 2$ is expected to increase as $\sim k_t^5$. Using these scalings, and for different truncation wave numbers, we normalized the results of Fig. 1. Figure 3 shows the number of $33 \rightarrow 3$ interactions normalized with k_t^6 and the number of $32 \rightarrow 3$ and $33 \rightarrow 2$ normalized with k_t^5. For sufficiently large Ro, the normalized curves are indistinguishable. In other words, for large Ro, there are no differences expected to arise between results in bounded domains and those in unbounded domains. Below a certain value of the nonlinear broadening, this scaling is weaker: the scaled curves differ from one another for small Ro. The discrepancy in the collapse of the scaled curves is particularly striking for the near-resonances $N_{33 \rightarrow 2}$. For example, $k_t = 20$ curve starts diverging from the larger k_t curve at $Ro \approx O(10^{-3})$. This is larger than Ro_{min} which was identified as threshold for 2D-3D decoupling. Hence, in the domains considered here, discreteness effects are increasingly important for a nonlinear broadening larger than Ro_{min}.

To summarize, in the present section we discussed the results of wave turbulence derived for unbounded domains. We examined whether these theoretical results (e.g., 2D-3D decoupling and freezing of the vertical energy transfers) would be observable in bounded domains. For domains typically used in numerical simulations we found and quantified a threshold Ro_{min} below which the assumptions behind the 2D-3D decoupling theories is valid in finite domains. We found and quantified a nonlinear broadening threshold Ro_c below which the vertical freezing prediction of Ref. [33] would be observable in bounded domains. A nonlinear broadening above Ro_c corresponds to a dynamics dominated by triple-wave interactions.

We investigated the discrepancies between the number of interactions resolved in unbounded and bounded domains (for a given truncation wave number). We found that for all dynamical regimes discussed (decoupling, vertical freezing, etc.), discreteness effects lead to differences between the number of near-resonances obtained in bounded and unbounded domains for relatively small Ro.

For the domains considered here, we found that discreteness effects become important for nonlinear broadenings larger than Ro_{min}. However, based on these results alone, we cannot determine this transition with more precision. We denote this transition nonlinear broadening as Ro_f, and now turn to a kinematic model of cascade in order to obtain a more precise assessment of Ro_f. Below Ro_f the dynamics could become significantly affected by discreteness effects.

IV. KINEMATIC MODEL

In his study of near-resonant capillary waves, Pushkarev [16] built two-dimensional maps (k_x, k_y) of modes satisfying the capillary three-wave near resonance. Using this, he
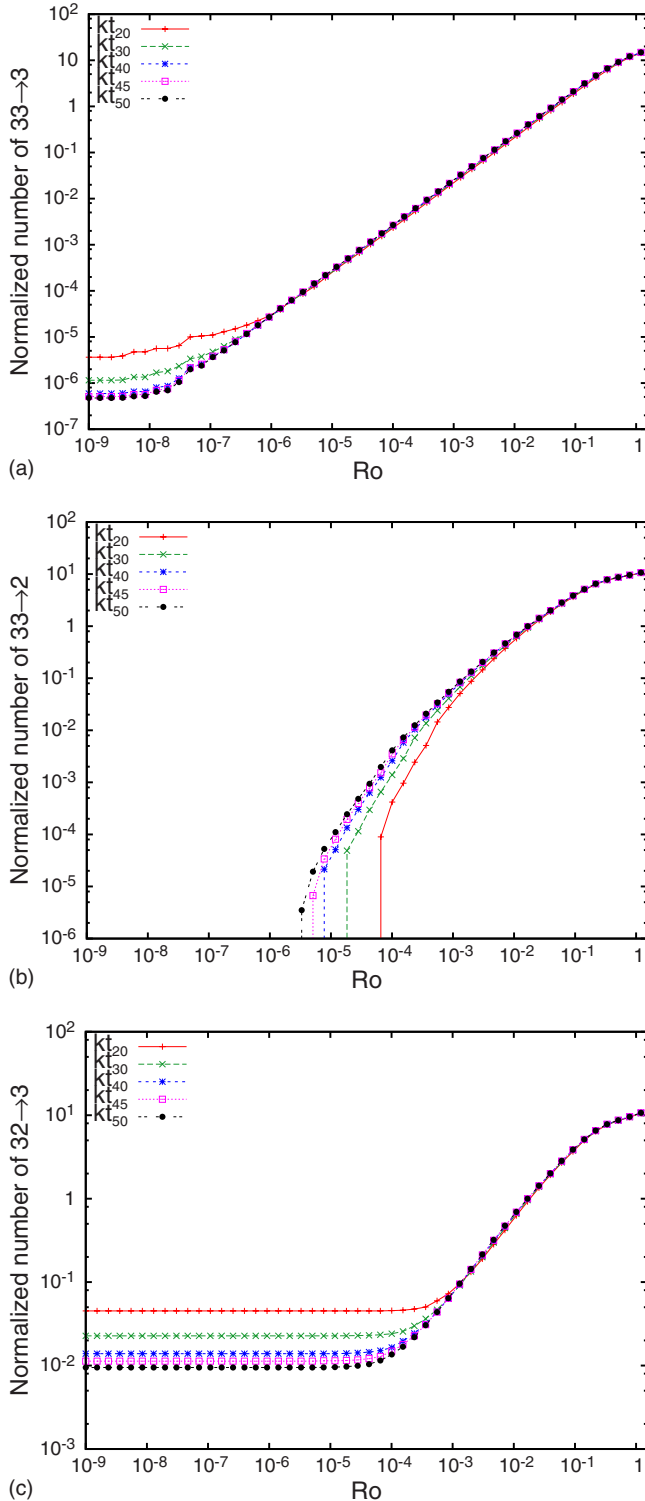
FIG. 3. (Color online) Effect of the discreteness on the variation of the number of resonant and near-resonant $33\rightarrow3$, $33\rightarrow2$, and $23\rightarrow3$ as a function of nonlinear broadening Ro. The number of $33\rightarrow3$ interactions are normalized with k_t^6 and the number of $32\rightarrow3$ and $33\rightarrow2$ normalized with k_t^5.

showed that the density of active modes changed significantly with the nonlinear broadening [17]. A kinematic model was proposed by Ref. [17] to study the discreteness effect on the transfer of energy via near-resonant capillary

waves. They started from an initial map of excited or activated modes, then given a level of nonlinear broadening, obtained subsequent maps of activated modes interacting with the initial set. The series of subsequent sets of active modes satisfied the near-resonant condition. This approach allowed them to determine the nonlinear broadening threshold below which no energy cascade could occur in a discrete spectral space.

Following a similar approach, we construct an iterative kinematic model of energy cascade through near-resonant inertial wave interactions (14). The dispersion relation of inertial waves is anisotropic and we therefore distinguish between the vertical and the horizontal wave numbers. The map of modes is constructed for three-dimensional wave numbers (k_x, k_y, k_z). We consider a discrete spectral domain of truncation k_t and start by assuming that only the modes in the initial set S_0 are active. For a given value of nonlinear broadening Ro, we construct the set of modes $\mathbf{k}$ of generation 1, S_1 such that $\mathbf{k} \in S_1$ if $\mathbf{k} \in S_0$ or

$$\mathbf{k} + \mathbf{k}_1 + \mathbf{k}_2 = 0 \quad \text{and} \quad |\omega_{s_\mathbf{k}} + \omega_{s_{\mathbf{k}_1}} + \omega_{s_{\mathbf{k}_2}}| \leqslant \text{Ro}$$

$$\text{with } (\mathbf{k}_1, \mathbf{k}_2) \in S_0 \times S_0. \tag{15}$$

That is, S_1 includes all modes $\mathbf{k}$ interacting with two modes of S_0 through near-resonances and with at most one zero interacting coefficient and $S_0 \subset S_1$. The procedure can then be repeated using S_1 as the initial set of active modes. We obtain successive generations of active modes $S_0, \ldots, S_n, \ldots, S_N$. The last set S_N includes all the modes that were activated by the cascade. All the sets with $n > N$ are identical to S_N, i.e., they do not contain any new activated modes. When S_N is reached, there are two possibilities. The first is that S_N contains all available modes of the domain. In other words, the propagation of the initial excitation reaches all modes. The second possibility is that not all the modes of the domain are contained in S_N, thus a subset of modes does not participate in the dynamics. Hence, discreteness effects clearly are present and can compromise numerical representation of the dynamics in the domain considered. In this last case, we say that the cascade is halted or that a freezing of the kinematic model cascade is taking place.

In addition to the general propagation of active modes throughout the spectral domain, we are also interested in investigating the role played by the various types of near-resonant interactions described in Table I. When going through the interactive steps described in Eq. (15) we also test for the type of modes involved ($V_\mathbf{k}$ or $W_\mathbf{k}$). For the $22 \rightarrow 2$ and $33 \rightarrow 3$ interactions we further require all three interaction coefficients to be nonzero. The $32 \rightarrow 3$ interactions have at least one nonzero interaction coefficient. Finally, the 2D interaction coefficient of the $33 \rightarrow 2$ interaction is non-zero.

We investigated two sets of initial modes: S_{0a} and S_{0b}. S_{0a} was chosen such that $|\mathbf{k}| \leqslant 5$ and contains a small number (424) of modes (Fig. 4 top panels). As such, this series S_{na}, $n = 0, 1, 2, \ldots$, mimics a forward cascade in a spectral domain. S_{0b} contains 2856 modes and is defined by $S_{0b} = \{\mathbf{k}: 11 < |\mathbf{k}| \leqslant 12\}$ in order to mimic a cascade initiated with a forcing at intermediate to small spectral scales.
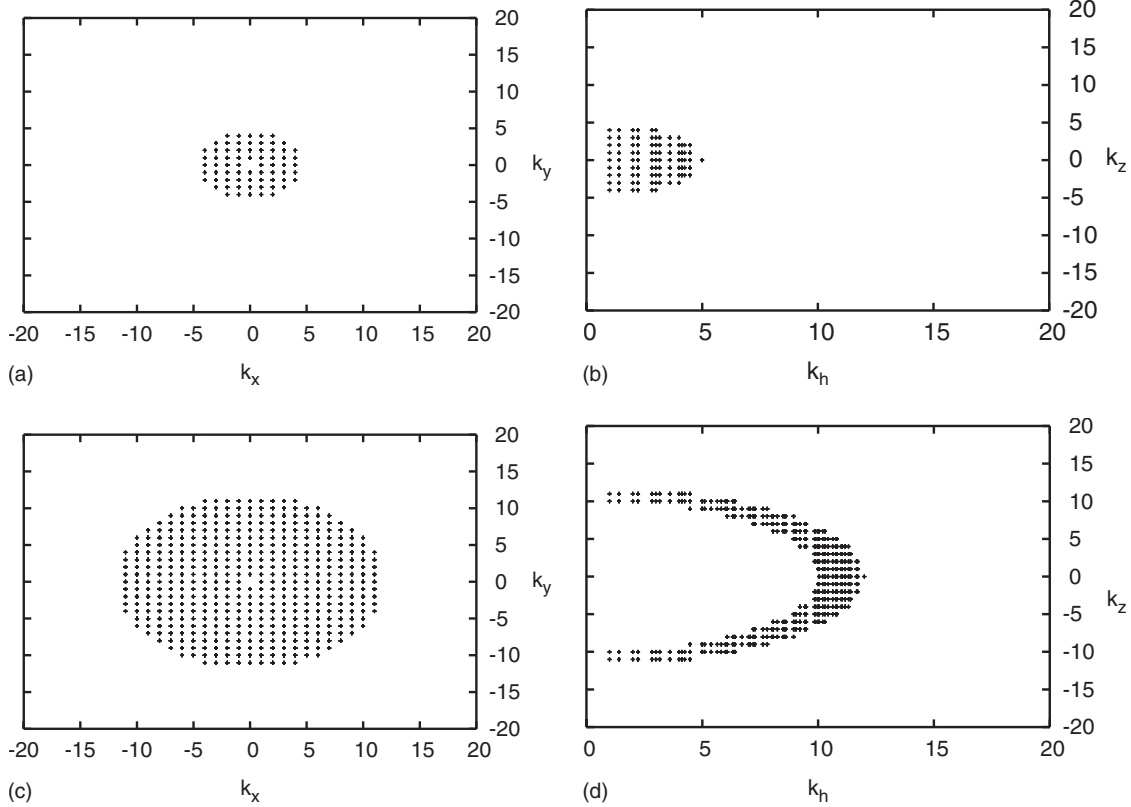
FIG. 4. Initial maps of active modes S_{0a} (top panel) and S_{0b} (bottom panel). Here the domain is truncated at $k_t=20$. The map of the horizontal components of the active modes are shown on a k_x-k_y plane (left panel) and the vertical components of the active modes on a k_h-k_z plane (right panel).

Figure 5 shows the maximum number of generations in the kinematic model when initialized with S_{0a} and for k_t =20. For small values of the nonlinear broadening, the sequence is frozen after three generations. At Ro=Ro$_f \approx 5.95 \times 10^{-4}$, there is an abrupt transition. For Ro larger than this "freezing" threshold, S_{Na} includes all modes. For Ro only marginally larger than Ro$_f$, a larger number of generations
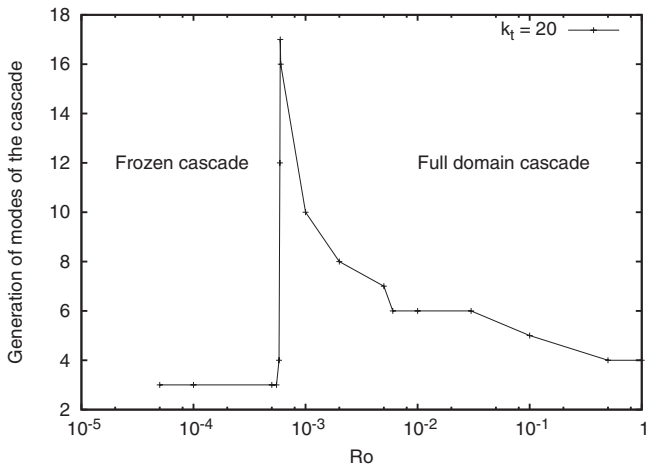

FIG. 5. Maximum number of iterations N of generation in the sequence S_{an} initiated with S_{0a} and for k_t=20. For a nonlinear broadening less than about 6×10^{-4} the series was frozen after a few interactions. For larger Ro, S_{Na} included all modes.

are needed before this occurs. Nevertheless, for all Ro $>$Ro$_f$ all modes are eventually activated and we conclude that discreteness effects are not precluding an energy cascade. It is also noteworthy that Ro$_f$ appears to be only weakly dependent on resolution. For example, a doubling of k_t resulted in only a small decrease in Ro$_f$, i.e., from Ro$_f$ $=5.95 \times 10^{-4}$ for k_t=20 to Ro$_f$=5.87×10^{-4} for k_t=40. It thus appears that, at least in this instance, discreteness effects become problematic at Ro considerably larger than Ro$_{min}$. However, the Rossby numbers typically used in simulations (e.g., 10^{-2}) are comfortably larger than Ro$_f$.

As was the model of Ref. [17], our model is kinematic only. It does not give information about the direction of exchange of energy between modes involved. However, from previous numerical studies of rapidly rotating turbulence, we know that modes with low linear frequencies receive energy preferentially. These correspond to modes with $k_h \gg k_z$. Also, in the decaying numerical simulations of Ref. [7], horizontal 3D energy transfers were more efficient than 3D energy vertical transfers. It is interesting that the kinematic model shows a similar anisotropy. That is, fewer generations are needed before all horizontal wave numbers are excited, whereas more are needed to excite all available vertical wave numbers. This is shown in Fig. 6, which plots the maximum horizontal and vertical wave numbers reached at each generation for various values of Ro and for both resolutions 64^3 and 100^3.

The point is further illustrated in Fig. 7, which shows the horizontal and vertical modes activated for the first few gen-
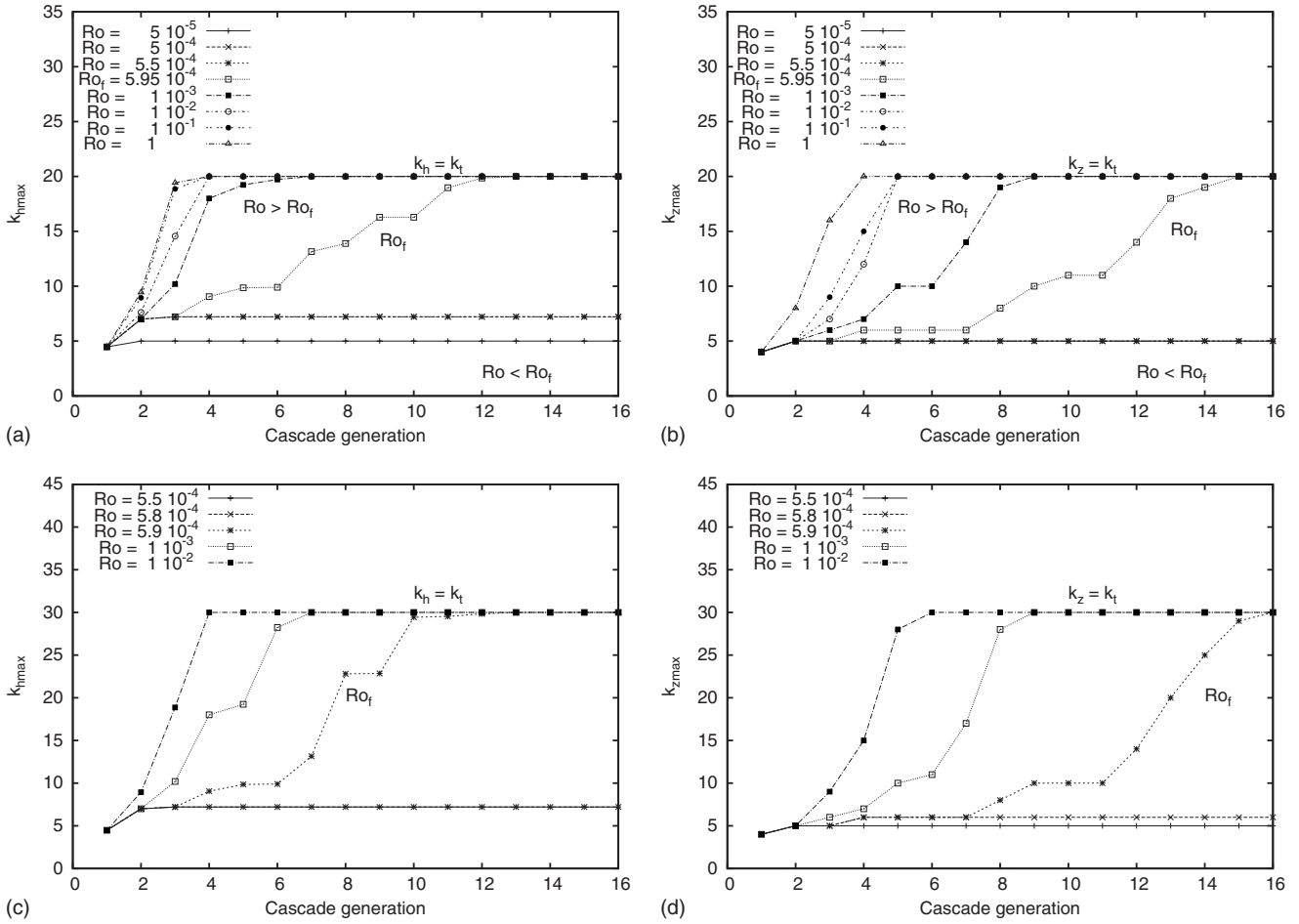
FIG. 6. Maximum horizontal (left panel) and vertical (right panel) wave numbers at each step of the cascade generation initiated with the set of excited modes S_{0a}, and for a domain of $k_t=20$ (top panel) and $k_t=30$ (lower panel). The critical freezing nonlinear broadening is the smallest Ro value to allow the cascade to extend to the smallest horizontal and vertical scales of the domains.

erations of the kinematic model initialized with S_{0a} and for $k_t=20$. It is clear that large horizontal wave numbers are activated prior to the activation of large vertical wave numbers. This anisotropy is visible in both the $33 \rightarrow 3$ and the $32 \rightarrow 3$ interactions. However, the $33 \rightarrow 3$ interactions lead to a faster excitation (i.e., an excitation in fewer iterations of the kinematic model) than the $32 \rightarrow 3$ interactions. As an illustration, we display the paucity of S_{Na} for a case where $\mathrm{Ro} < \mathrm{Ro}_f$ for which the propagation was halted at $N=3$ in Fig. 8. Finally, $22 \rightarrow 2$ interactions do not show any freezing of the propagation of the excitation among 2D modes (not shown). In fact, the propagation of the active modes among the set of 2D modes always takes only three generations.

V. DISCUSSION AND CONCLUSION

The discreteness of wave numbers in a periodic domain has proven to be at the origin of the freezing of the nonlinear transfers between modes dominated by resonant capillary wave interactions. A similar effect was also suspected in rotating turbulence. In contrast to capillary waves, however, inertial waves can satisfy the resonant condition for integer-value wave numbers, suggesting that a freezing might not occur in that system.

We studied the discreteness effects in order to clarify this issue. The discreteness effects are twofold. One aspect is the integer-valued wave numbers, i.e., the finiteness intrinsic property of bounded domains versus unbounded domains. The other aspect is the resolution used in a particular bounded domain of interest. We examined how the reduction of the nonlinear broadening Ro affects the distribution and number of resonant and near-resonant interactions on a range of Ro in periodic domains relevant for numerical studies. We constructed a kinematic model of resonant and near-resonant interactions and used it to show that discreteness effects are detected for small nonlinear broadenings. We also showed that, as with capillary waves, a freezing of the energy transfers is also possible in discrete inertial waves, provided Ro was sufficiently small. This latter effect was not sensitive to a change of resolution.

Concerning the decoupling between the dynamics of the 2D and 3D modes predicted for the limit of $\mathrm{Ro} \rightarrow 0$, we showed the existence of a minimum nonlinear broadening Ro_{min} below which 3D-2D interactions do not exchange energy. In a continuous domain, only the $\mathrm{Ro}=0$ limit strictly prevents the resonant 3D-2D interactions from exchanging energy. However, in a discrete domain, this value is nonzero. We quantified Ro_{min} for different resolutions. For example,
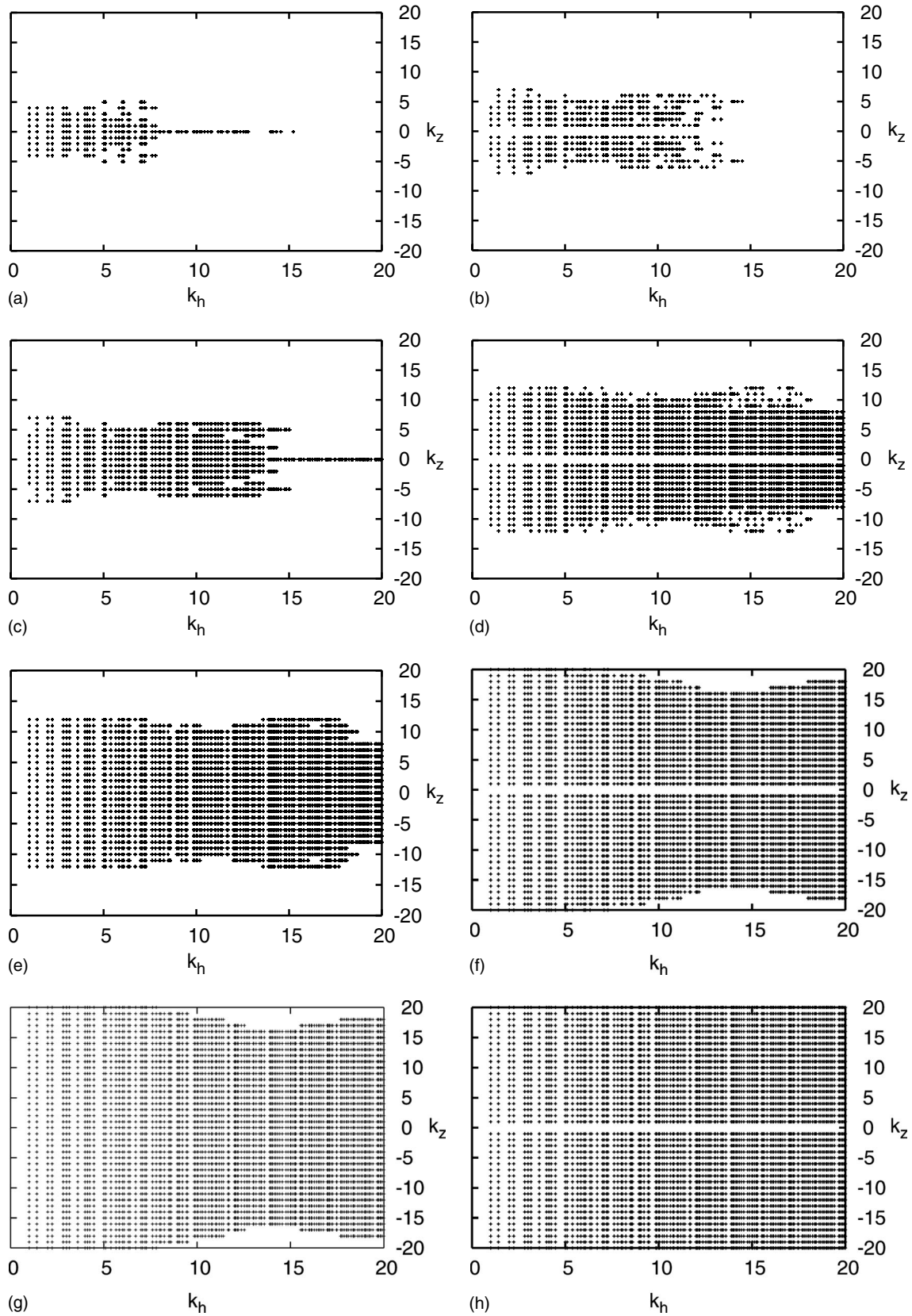
FIG. 7. k_h-k_z maps of modes activated at generations S_2 (top panel) to S_5 (bottom panel) by the $32 \rightarrow 3$ interactions (left panel) and the $33 \rightarrow 3$ interactions (right panel) with Ro=0.01, k_t=20 and initial active modes S_{0a} (see Fig. 4). The final state of the cascade corresponds to the activation of all the modes of the domain.
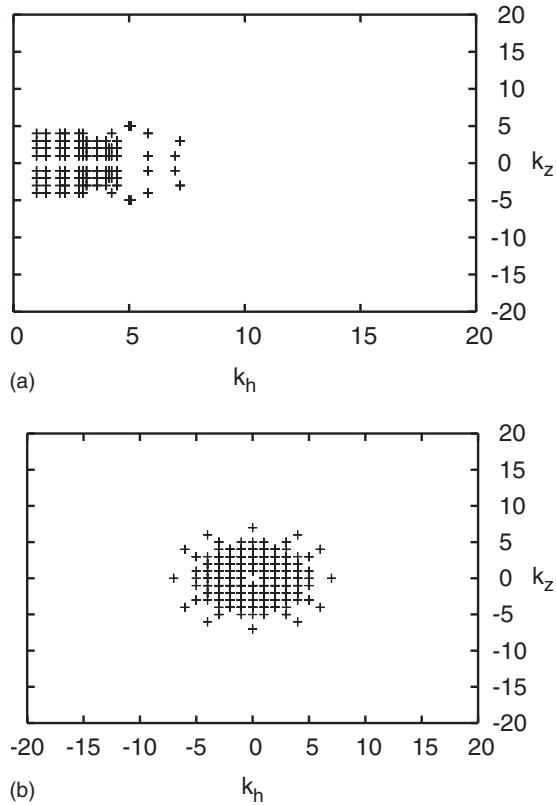
FIG. 8. Maps of the modes of generation S_{Na}, with $N=3$ at which the cascade is halted when Ro$=5.5\times10^{-4}$ and $k_t=20$.

Ro_{min} varies from $Ro_{min}=6.6\times10^{-5}$ for a resolution 64^3 to $Ro_{min}=3.3\times10^{-6}$ for a resolution 166^3. Thus, a resolution of 128^3 with a minimum nonlinear broadening of $Ro<Ro_{min}=7.8\times10^{-6}$ would automatically show a decoupling between the 3D and the 2D modes.

In addition, another threshold of nonlinear broadening is found and denoted Ro_c. For $Ro<Ro_c$, the number of $32\rightarrow3$ interactions is larger than the triple wave ($33\rightarrow3$) interactions. In this regime, the freezing of the vertical energy transfers predicted by Ref. [33] would be possible. Above Ro_c no such regime would be possible. The kinematic model also showed that both $32\rightarrow3$ and triple wave interactions ($33\rightarrow3$) favor the propagation of the cascade to small horizontal scales and large vertical scales. We find that it takes a smaller number of generations for these interactions to excite the maximum horizontal wave numbers of the domain compared to the number of generations needed to reach the maximum vertical wave numbers. This reinforces wave-turbulence's prediction of anisotropy and concentration of energy into small inertial frequency modes.

We found a regime of freezing of energy transfers to be present in the system of inertial waves. We quantified the threshold nonlinear broadening Ro_f below which no energy cascade develops throughout the entire domain. Ro_f depends on the initial set of excited modes (scale of the forcing). Surprisingly, it only varies slightly with changes of domain resolution. The kinematic model showed that a simulation in a domain with a resolution of about 64^3 would not be subject to an energy transfer freezing except for nonlinear broadening values Ro_f as small as 5.95×10^{-4}. This threshold de-

creases only slightly to $Ro_f=5.87\times10^{-4}$ for a resolution of 133^3. These values of Ro_f are much smaller than Rossby numbers used in most numerical simulations of rotating turbulence.

The existence of the Ro_f threshold and existence of exact resonances in discrete domains is reminiscent of water-wave systems, where an interesting discreteness phenomenon is seen in a weakly forced setting [20]. In that system energy was observed to accumulate around the forcing scale until the nonlinear broadening of resonant interactions attained a critical value sufficient to overcome the discreteness of the modes. This was followed by a sudden discharge or "avalanche" of energy in the form of an energy cascade after which the system oscillated between stages where the energy builds up and stages where it is discharged [21]. Weak forcing of inertial wave turbulence could lead to a similar oscillation. We would observe alternating phases: a freezing in which energy builds up until Ro reaches Ro_f, above which a phase of energy transfers could then occur. This would need further investigation of forced rotating flows with $Ro\approx Ro_f$.

In the domains examined here, we found that $Ro_f>Ro_{min}>Ro_c$. From a practical standpoint, this implies that dynamical theories related to the properties of the resonances alone—that is the decoupling theories and the vertical energy freezing—would not be applicable in simulations with $Ro>Ro_f$, for which the number of interactions scale as in an infinite domain. In other words, if a decoupling or a reduced vertical energy transfer is observed in these domains, they are intrinsic dynamical properties of the flow in the bounded domain considered. We showed that these features cannot be directly explained by the results on continuous resonance interactions and especially cannot be explained by the notion that discreteness effects do not allow for some interactions to be resolved.

When carrying out simulations and considering Ro_f, it is important to use the relevant definition of Ro. Several definitions of Rossby numbers are used in the literature. Some calculate Ro based on the forcing scale, which guarantees a constant value. Some use a Rossby number based on the statistics of the evolving flow. These include, for example, the mean velocity or vorticity [29]. As an illustration, consider the example of Ref. [13], who estimated their Ro based on the forcing of the flow. They obtained a $Ro=8.6\times10^{-2}$. However, they found that a reduced model of near-resonances calculated using $Ro\approx2.58\times10^{-2}$ (in 14) better reproduced the increase of 2D energy of the full flow. Using their full-simulation spectra (Fig. 3), we estimate that their most energy containing scale (larger scale) has a macro-Rossby of $Ro=U/2\Omega L\approx0.0255$. This value matches the nonlinear broadening 0.0258 of the near-resonances found to reproduce better the dynamics of the full equations. This suggests that when comparing Ro of simulations with values such as Ro_f or Ro_{min} identified in our study, one should consider that the relevant Ro is that obtained from averaged velocity or vorticity quantities of the evolving flow (e.g., macro-Ro or micro-Ro). Note that Ref. [7] found that the macro and micro Ro were equivalent in the intermediate Ro regime simulations, where energy is concentrated in the larger scales of the flow, this is not the case for other rotating regimes, such as the small or large Ro regimes.

In sum, given the relatively small value of Ro_f and its weak dependence on resolution, we submit that most numerical simulations on rotating turbulence carried out so far would have been free of discreteness effects. However, it is important for future studies of rotating turbulence to assess in which kinematic regime they fall. This can be done by comparing their Ro with the thresholds identified in this paper taking into account the domain of study considered. When comparing the Rossby number of a simulation to the freezing Ro estimated in this study, the relevant definition of Rossby number is that related to the averaged evolving quantities of the flow.

ACKNOWLEDGMENTS

[1] H. P. Greenspan, *The Theory of Rotating Fluid* (Cambridge University Pres, Cambridge, 1968).

[2] G. I. Taylor, Proc. R. Soc. London, Ser. A **104**, 213 (1923).

[3] A. D. McEwan, Nature (London) **260**, 126 (1976).

[4] C. N. Baroud, B. B. Plapp, Z. S. She, and H. L. Swinney, Phys. Rev. Lett. **88**, 114501 (2002).

[5] J. Bardina, J. H. Ferziger, and R. S. Rogallo, J. Fluid Mech. **154**, 321 (1985).

[6] P. Bartello, O. Métais, and M. Lesieur, J. Fluid Mech. **273**, 1 (1994).

[7] L. Bourouiba and P. Bartello, J. Fluid Mech. **587**, 139 (2007).

[8] M. Hossain, Phys. Fluids **6**, 1077 (1994).

[9] P. K. Yeung and Y. Zhou, Phys. Fluids **10**, 2895 (1998).

[10] L. M. Smith and F. Waleffe, Phys. Fluids **11**, 1608 (1999).

[11] Q. Chen, S. Chen, G. L. Eyink, and D. D. Holm, J. Fluid Mech. **542**, 139 (2005).

[12] A. C. Newell, J. Fluid Mech. **35**, 255 (1969).

[13] L. M. Smith and Y. Lee, J. Fluid Mech. **535**, 111 (2005).

[14] E. A. Kartashova, Phys. Rev. Lett. **72**, 2013 (1994).

[15] E. Kartashova, in *Nonlinear Waves and Weak Turbulence*, edited by V. E. Zakharov (American Mathematical Society, Providence, R.I., 1998), pp. 95–129.

[16] A. Pushkarev, Eur. J. Mech. B/Fluids **18**, 345 (1999).

[17] C. Connaughton, S. Nazarenko, and A. Pushkarev, Phys. Rev. E **63**, 046306 (2001).

[18] M. Tanaka and N. Yokoyama, Fluid Dyn. Res. **34**, 199 (2004).

[19] V. E. Zakharov, A. O. Korotkevich, A. N. Pushkarev, and A. I. Dyachenko, JETP Lett. **82**, 544 (2005).

[20] Y. V. Lvov, S. Nazarenko, and B. Pokorni, Physica D **218**, 24 (2006).

[21] S. Nazarenko, J. Stat. Mech.: Theory Exp.(2006) L02002.

[22] S. Nazarenko, New J. Phys. **9**, 307 (2007).

[23] F. Bellet, F. Godeferd, J. Scott, and C. Cambon, J. Fluid Mech. **23**, 81 (2006).

[24] C. Cambon, N. N. Mansour, and F. S. Godeferd, J. Fluid Mech. **337**, 303 (1997).

[25] L. Bourouiba, Phys. Fluids **20**, 075112 (2008).

[26] C. Morize and F. Moisy, Phys. Fluids **18**, 065107 (2006).

[27] A. Ibbetson and D. J. Tritton, J. Fluid Mech. **68**, 639 (1975).

[28] G. P. Bewley, D. P. Lathrop, L. R. M. Maas, and K. R. Screenivasan, Phys. Fluids **19**, 071701 (2007).

[29] L. Jacquin, O. Leuchter, C. Cambon, and J. Mathieu, J. Fluid Mech. **220**, 1 (1990).

[30] F. Waleffe, Phys. Fluids A **4**, 350 (1992).

[31] F. Waleffe, Phys. Fluids A **5**, 677 (1993).

[32] A. Babin, A. Mahalov, and B. Nicolaenko, Eur. J. Mech. B/Fluids **15**, 291 (1996).

[33] A. Babin, A. Mahalov, and B. Nicolaenko, Theor. Comput. Fluid Dyn. **11**, 215 (1998).

[34] C. Cambon, R. Rubinstein, and F. S. Godeferd, New J. Phys. **6**, 73 (2004).

[35] E. Kartashova, Phys. Rev. Lett. **98**, 214502 (2007).

[36] J. P. Boyd, *Chebyshev & Fourier Spectral Methods* (Springer-Verlag, Berlin, 1989).

[37] W.-C. Müller and M. Thiele, Europhys. Lett. **77**, 34003 (2007).

[38] S. Galtier, S. Nazarenko, A. C. Newell, and A. Pouquet, J. Plasma Phys. **63**, 447 (2000).

[39] The intermediate regime in decaying turbulence share most of the properties observed in forced turbulence simulations restricted to near-resonant interactions such as used in Ref. [13]. The existence of this regime is certainly due to the particular property of near-resonant interactions for this range of Ro.